IEEE Photonics Journal
An IEEE Photonics Society Publication

Open Access

Cascaded Microwave Photonic Filters for Side Mode Suppression in a Tunable Optoelectronic Oscillator applied to THz Signal Generation and Transmission

Volume 13, Number 1, February 2021

G. K. M. Hasanuzzaman, *Student Member, IEEE*
Haymen Shams, *Member, IEEE*
Cyril C. Renaud, *Senior Member, IEEE*
John Mitchell, *Senior Member, IEEE*
Alwyn J. Seeds, *Fellow, IEEE*
Stavros Iezekiel, *Senior Member, IEEE*

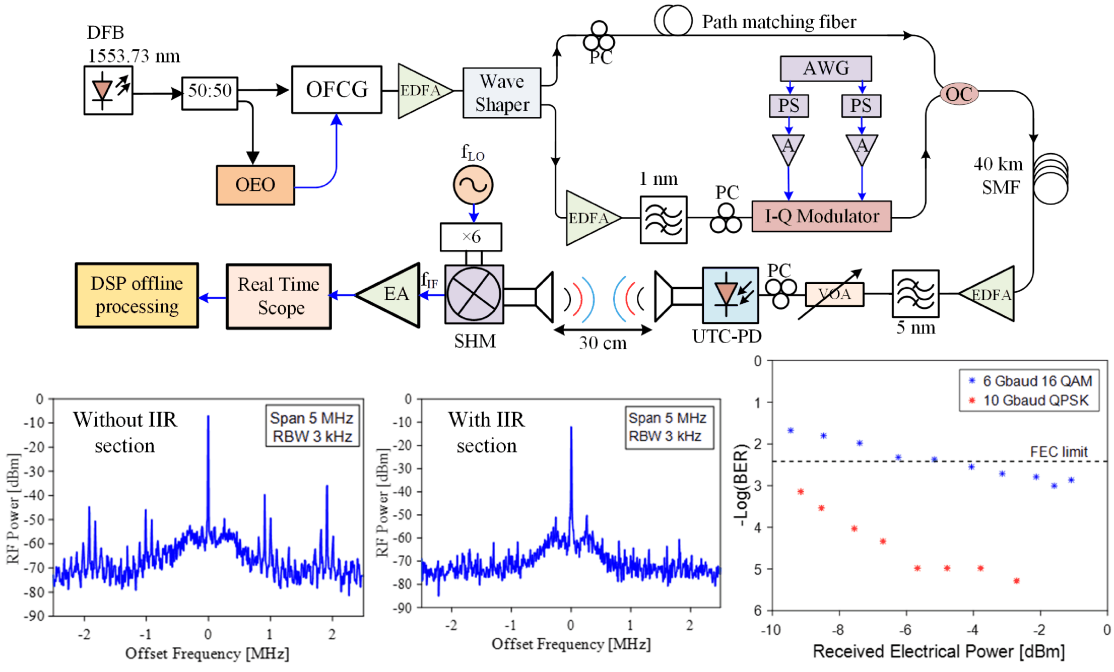

DOI: 10.1109/JPHOT.2020.3044342

Cascaded Microwave Photonic Filters for Side Mode Suppression in a Tunable Optoelectronic Oscillator applied to THz Signal Generation and Transmission

G. K. M. Hasanuzzaman [1,2] ***Student Member, IEEE***,
Haymen Shams [3] ***Member, IEEE***,
Cyril C. Renaud [3] ***Senior Member, IEEE***,
John Mitchell [3] ***Senior Member, IEEE***,
Alwyn J. Seeds [3] ***Fellow, IEEE***,
and Stavros Iezekiel [1] ***Senior Member, IEEE***

[1]Microwave Photonics Research Laboratory, EMPHASIS Research Centre, University of Cyprus, Nicosia 1678, Cyprus
[2]Department of Electrical and Electronic Engineering, Rajshahi University of Engineering and Technology, Kazla, Rajshahi 6204, Bangladesh
[3]Department of Electronic and Electrical Engineering, University College London,Torrington Place, London WC1E 7JE, U.K.

DOI:10.1109/JPHOT.2020.3044342

Manuscript received November 12, 2020; accepted December 7, 2020. Date of publication December 14, 2020; date of current version January 5, 2021. This work was supported by European Union's Horizon 2020 research and innovation programme under Grant 642355. Corresponding author: Stavros Iezekiel (e-mail: iezekiel@ucy.ac.cy).

Abstract: We demonstrate experimentally an optoelectronic oscillator (OEO) in which high side-mode suppression is achieved by cascading a phase modulator-based single pass-band tunable microwave photonic (MWP) filter with an optoelectronic feedback loop-based infinite impulse response (IIR) MWP filter. The OEO provides an RF oscillation that can be tuned from 6.5 GHz to 17.8 GHz with a phase noise lower than -103 dBc/Hz. Experimental results show that inclusion of the IIR section leads to a 20 dB reduction of phase noise close to the carrier and an increase of 10 dB in side mode suppression, compared to the equivalent OEO without an IIR section. The OEO was used to drive an optical frequency comb generator to generate a THz signal at 242.6 GHz by optical heterodyning; inclusion of the IIR section increases suppression of the side modes neighboring the THz carrier. A radio over fiber link was then implemented at a 242.6 GHz carrier frequency, with transmission of a 24 Gbps signal over 40 km of fiber and a 30 cm wireless path at a bit error rate below the forward error correction limit. The proposed system may be applied to frequency reconfigurable THz links and radars.

Index Terms: Microwave photonics, optoelectronic oscillator, side mode suppression, infinite impulse response.

1. Introduction

Optoelectronic oscillators (OEO) [1], [2] have many applications due to their low phase noise, including microwave signal generation, instrumentation [3], sensing [4], radar systems and frequency down conversion [5]. In particular, tunable OEOs with high side mode suppression, low

phase noise, and wideband frequency tunability are of interest for radar detection of slow-moving targets. Due to the inherent multimode nature of an OEO, electrical bandpass filters (EBPF) are used to define the oscillation frequency. However, an EBPF is unable to maintain mode-hopping free and single mode operation since its passband is broader than the free spectral range (FSR) of a long-cavity OEO. For example, a 2 km fiber provides an FSR of 100 kHz, but a microwave EBPF with such a narrow passband, minimal drift of center frequency (with temperature and vibration) and frequency tuning capability is difficult to realize. Although yttrium iron garnet (YIG) filters can be tuned up to 50 GHz, their frequency accuracy is limited to several tens of MHz and their bandwidth is not sufficiently narrow to ensure spur-free oscillation [6].

In [7], a side mode suppressed tunable OEO was implemented using an EBPF and injection locking (via an external electrical synthesizer), but the tuning range (from 8.5 to 9.5 GHz) was limited to the passband of the electrical bandpass filter. In contrast, microwave photonic (MWP) filters offer tunability over a greater frequency range than their electrical counterparts and have been used in a number of recent OEOs [7].

There are two types of MWP filter: those with a single passband, and those with periodically repeating passbands. The latter, which may be implemented with either a finite impulse response (FIR) or an infinite impulse response (IIR), provide a high Q factor, but the periodic response is unsuitable for an OEO [8]. One approach to achieve both high selectivity and a high Q factor is to cascade a single passband filter with a periodic spectral response filter - either FIR or IIR. Of the two, the IIR implementation requires fewer components than the FIR, but in an all-optical IIR filter the issue of optical coherence can lead to environmentally sensitive performance. This may be overcome with a hybrid optoelectronic loop, in which phase-induced intensity noise (PIIN) is mitigated through consecutive E/O and O/E conversions in the loop [9], [10]. By cascading a single passband filter with an optoelectronic IIR section, the single passband section determines the center frequency of oscillation and the IIR section provides the high Q filtering for side mode suppression. This topology was used in [11] with an EBPF and an optoelectronic IIR section, to produce an OEO with side mode suppression of 93 dB at 29 GHz. However, this OEO lacked frequency tunability. In [12], a tunable OEO incorporating a simulated Brillouin scattering (SBS) based tunable MWP filter and an active recirculating delay lined based IIR filter was reported. A side mode suppression of 95 dB and a tuning range of DC to 40 GHz was achieved. In [13], we demonstrated a tunable OEO based on a single passband MWP, which was then used to drive an optical frequency comb generator (OFCG) for generation of mm-wave and THz signals. A phase modulator (PM) and a tunable optical bandpass filter (TOBF) combination were used to provide tunability of the MWP filter, which was subsequently used to provide tunable electrical oscillation from 6.5 GHz to 18.36 GHz with a phase noise $<$-103 dBc/Hz at an offset of 10 kHz and side mode suppression ratio (SMSR) 65 dB. We generated signals at 101.5 GHz and 242.6 GHz by two tone selection and optical heterodyning. However, we found that the side modes in the microwave signal (from the driving OEO) are translated and more pronounced in the mm-wave and THz signals from the OFCG.

In this paper, we modify the tunable dual-loop OEO architecture [13] by cascading the single passband MWP filter of that topology with an additional optoelectronic IIR MWP filter section (Fig. 1), in order to increase the SMSR both in the microwave and THz band. Experimental results show that by incorporating the IIR section, the SMSR is increased by 10 dB, the close to carrier phase noise is reduced by 20 dB and the stability of the OEO is improved by a factor of ten, to 6×10^{-9}. We compare our OEO design with other topologies in Table I, where it is seen that our approach provides better side mode suppression except for the dual injection locked OEO topology [14]. However, unlike our OEO, the one in [14] is fixed in frequency.

We then proceed to use the OEO to drive an OFCG, and through two-tone selection via a wavelength selective switch (WSS) and subsequent optical heterodyning in a uni-traveling carrier photodiode (UTC-PD), a THz signal at 242.6 GHz is generated. Upon down-converting this THz signal and by incorporating the additional IIR section, the side modes are less pronounced than the corresponding results in [13]. Additionally, we have developed a radio over fiber (RoF) link based on this topology for which a 6 Gbaud 16 QAM modulated 242.6 GHz carrier was transmitted over

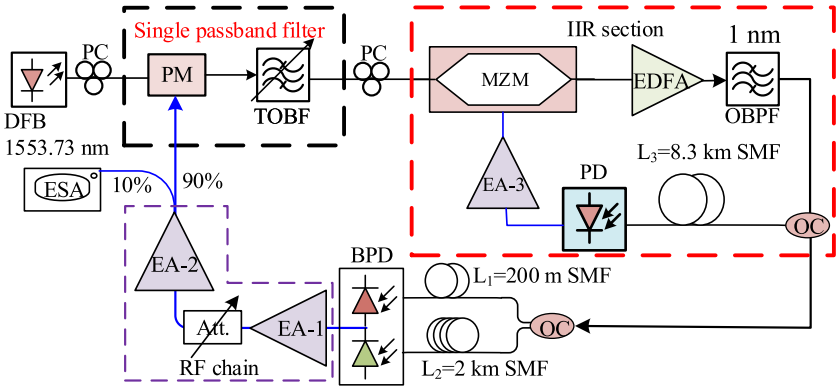

Fig. 1. Experimental set-up of the proposed tunable OEO. The black dotted section represents the single passband MWP filter and the red dotted section represents the IIR MWP filter.

TABLE 1

Comparison of OEO Topologies for Side-Mode Suppression. FP: Fabry Perot, MWP: Microwave Photonic, FQM: Frequency Quality Multiplier, DSF: Dispersion Shifted Fiber. It Is To Be Noted That Side Mode Suppression Is Calculated from the Phase Noise Curve

Ref.	OEO Topology	Frequency of oscillation	No. of fiber loops	Fiber lengths	SSB phase Noise @ 10 kHz	Side mode suppression	Comments
[15]	Dual-loop OEO	12 GHz	Dual	10 km/ 5.5 km	-109 dBc/Hz	100 dB	Fixed in frequency. First and widely used photonic technique for side mode suppression. The resultant Q of the combined loop is lower than that of long loop.
[16]	OEO with FP etalon	10.5 GHz	Single	2 km	-105 dBc/Hz	105 dB	No electrical filter is required. The oscillation frequency is determined by the FSR of the FP etalon. As a result, frequency tunability is only possible for multiples of the FSR.
[11]	OEO with cascaded RF and MWP filter.	29.99 GHz	Single	3 km DSF	-113 dBc/Hz	83 dB	OEO scheme is simple and easy to implement and control. Fixed in frequency.
[17]	OEO with FQM	3 GHz	Single	15 km	-140 dBc/Hz	120 dB	Fixed in frequency. Requires proper tuning of the FQM parameters. Phase noise increases due to the noise factor increased by the FQM.
[14]	Dual injection locked OEO.	10 GHz	Two single loops	6 km, 50 m	-150 dBc/Hz	140 dB	Two separate OEOs are required. Frequency and power fluctuation of master loop effects the performance of the slave loop. Fixed in frequency.
[18]	Injection locked OEO with low frequency RF signal.	20 GHz	Single	3 km	-110 dBc/Hz	90 dB	Requires an optoelectronic system to generate the high frequency RF from the low frequency RF. Fixed frequency oscillation.
This work	OEO with cascaded MWP filter.	17.33 GHz	Dual	2 km/ 200 m	-103 dBc/Hz	125 dB	Frequency tunable; the phase noise can be further improved by using long length fiber and optimizing the RF components.

a 30 cm wireless distance with a bit error rate (BER) less than the forward error correction (FEC) limit.

The paper is organized as follows. The operating principle of the single passband and IIR MWP filter is discussed in Section 2, while in Section 3, the OEO based on the cascaded MWP filter is discussed. The experimental set-up, results and discussion on side mode suppressed THz signal generation are presented in Section 4. In Section 5, the experimental set-up of the RoF link is covered, while Section 6 concludes the work.

2. Principle of Operation of Cascaded MWP Filter Sections

2.1 Single Pass Band Tunable MWP Filter

The single passband tunable MWP filter consists of a PM and a tunable OBPF as shown in the black dotted portion of Fig. 1. A PM generates antiphase sidebands when modulated with an external RF carrier. If an optical band pass filter with a center frequency equal to the optical carrier frequency and a bandwidth equal to or wider than double the modulating RF frequency is placed after the PM, then when the anti-phase sidebands are photo-detected, a zero RF response is generated. However, if the center frequency of the optical carrier is slightly detuned from the center frequency of the optical filter, asymmetrical sideband suppression occurs. The photodiode will then generate a beating signal between the remaining unbalanced sideband and the optical carrier, giving a single sideband RF response. Therefore, the combination of phase modulator (PM) and the tunable optical bandpass filter (TOBF) acts, upon photodetection, as a single passband microwave photonic filter (MWPF). Here, the center frequency (f_0) in the electrical domain is half of the optical bandwidth (B) of the TOBF and the bandwidth (Δf) in the electrical domain is twice the offset between the center frequency of the TOBF (ω_0) and the laser oscillation frequency (ω_c) [8]. We can express these relationships as follows:

$$f_o = \frac{B}{2} \tag{1}$$

$$\Delta f \ = 2(\omega_c \ - \omega_o) \ = \ 2\Delta\omega. \tag{2}$$

where $\Delta\omega = (\omega_c \ - \omega_o)$ is the offset between the laser oscillation frequency and center frequency of the TOBF. The center frequency in the electrical domain (f_0) can be tuned by changing the bandwidth of the TOBF (B) according to equation (1); increasing the TOBF bandwidth leads to a corresponding increase in the center frequency of the MWPF. From equation (2), the bandwidth in the electrical domain (Δf) can be tuned by changing the offset between the center frequency of the TOBF (ω_0) and the laser oscillation frequency (ω_c). Bandwidth tuning can be realised either by changing the center frequency of the TOBF or laser oscillation frequency. Both the tuning parameters are mutually independent in principle.

2.2 Optoelectronic IIR MWP Filter

A first-order optoelectronic IIR MWP filter (the red dotted box of Fig. 1) is a feedback loop with an open loop gain less than unity [9], [19], [20]. It comprises a Mach-Zehnder modulator (MZM), an erbium doped fiber amplifier (EDFA) with an OBPF, a standard single-mode fiber (SMF) several kilometers in length, a high-speed photo-detector (PD), and an electrical amplifier. The quality factor (Q) and rejection ratio increase with higher loop gain (η). This in turn depends on the optical and electrical amplifier gain, MZM and PD optoelectronic conversion efficiency, and the input optical power to the IIR section. The IIR loop operates in the incoherent regime where the total loop delay (T) is greater than the laser diode coherence time, providing a periodic passband and stopband with a free spectral range (FSR) of $1/T$. A unique feature is that the MZM bias controls the position of the passband and stopband; for example, the stopband response may be swapped with the passband by switching from positive quadrature bias to negative quadrature [9].

3. Cascaded MWP Filter Based OEO

3.1 Experimental Arrangement

Fig. 1 shows the experimental arrangement of the cascaded MWP filter based OEO. Light from a distributed feedback (DFB) laser (RIO ORION laser module) operating at 1553.73 nm was passed through a single passband filter comprising a phase modulator (iXblue MPZ-LN-40) and a tunable optical bandpass filter (XTM-50, Option:Standard) as described in the previous section. We tuned the center frequency of the TOBF as close as possible to the laser oscillation frequency to keep the

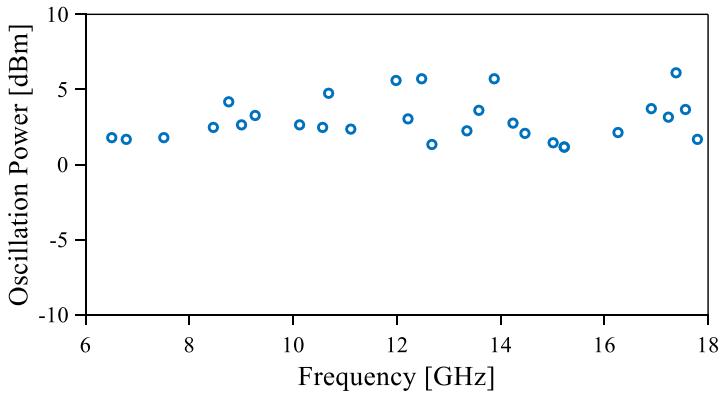

Fig. 2. Oscillation power plotted for different oscillation frequencies as the OEO is tuned from 6.5 GHz to 17.8 GHz.

resultant electrical filter bandwidth as narrow as possible. Apart from being an integral part of the tunable MWPF, the PM also functions as an electrical-to-optical (E/O) converter for the OEO loop [8]. The output of the single passband filter is then connected to the optoelectronic IIR section. In the IIR section, we used a MZM (JDS uniphase, model number:10024291) that works an an E/O converter. The modulated output of the MZM is then passed through an EDFA (Thorlabs, EDFA100S); the EDFA compensates the O/E and E/O conversion losses of the IIR loop and can thus control the loop gain. A 1 nm OBPF was placed immediately after the EDFA to reject the out-of-band amplified spontaneous emission (ASE) noise. The output of the OBPF is split into two paths by a 3 dB optical coupler, with one output being passed through an 8.3 km length of SMF, photo-detected in a high-speed photodiode (XPDV3120R, with a 3-dB bandwidth of 70 GHz, and DC responsivity of 0.60 A/W), electrically amplified (EA-3, Microsemi, AML618P3502-BT, 6–18 GHz) and finally connected to the RF port of MZM to complete the IIR loop. The other output of the coupler passes through a dual loop OEO section with short (L_1) and long (L_2) loop lengths of 200 m and 2 km, respectively. The optical output of the two fiber spools is fed to a balanced photodetector (DSC730, with a 3-dB bandwidth of 25 GHz, and responsivity of 0.60 A/W), with the photo-detected signal being amplified in order to compensate the O/E and E/O conversion losses of the main OEO loop. We used two amplifiers in the OEO loop; the first stage (EA-1, RF-Lambda RLNA00G30GA) operates between 0.01–30 GHz while the second stage (EA-2, Microwave Solutions MSH-748603) operates between 6–18 GHz. Between the two amplifier stages, we used an attenuator (Hewlett-Packard, 8494B, DC-18 GHz, 0 to 11 dB with 1 dB step) to avoid saturation; the attenuation factor was set between 0 to 11 dB at different oscillation frequencies since the gain of the amplifiers (EA-1 and EA-2) varies with frequency. Finally, a 10:90 electrical coupler is used for spectrum analysis (the 10% output is connected to a Rohde & Schwarz, R&SFSU26 electrical spectrum analyzer (ESA) while the remaining 90% is connected to the RF port of the PM to complete the OEO loop. Polarization controllers (PC) were used before the electro-optics modulators (PM and MZM) to minimize the polarization dependent loss.

3.2 Experimental Results and Discussion

The RF output signal of the OEO can be tuned from 6.5 GHz to 17.8 GHz by tuning the optical bandwidth of the TOBF of the single passband MWP filter section; the tuning range is limited by the bandwidth of the RF components of the OEO loop, and specifically the second amplifier (EA-2) in the OEO loop which operates between 6–18 GHz. The RF power of the oscillating signal at different OEO oscillation frequencies is illustrated in Fig. 2; oscillation power in excess of 0 dBm was obtained for the whole tuning range, with a ripple of the order of 5 dB. This ripple in the OEO output power of an OEO is due to the frequency dependence of the small signal loop gain [2],

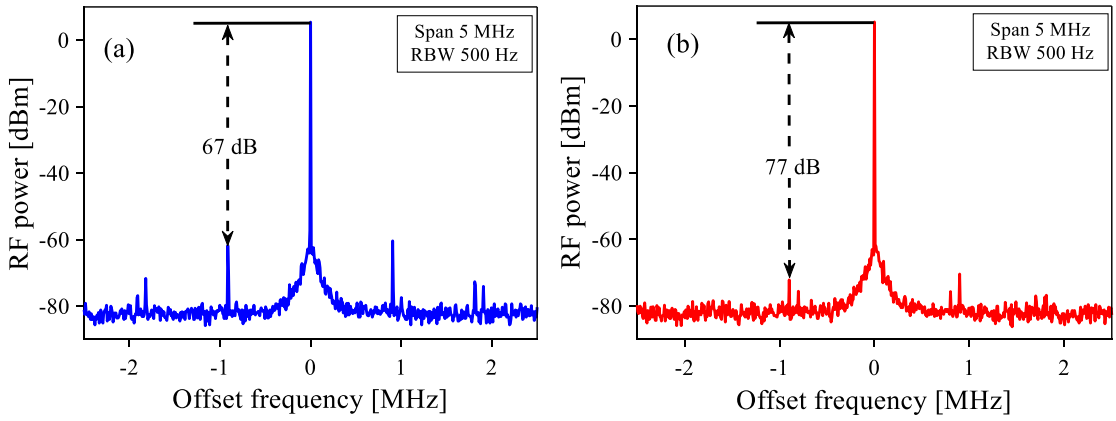

Fig. 3. Electrical spectra of the generated RF signal using the tunable OEO at 17.33 GHz. (a) without the IIR section (b) with the IIR section. There is an improvement in SMSR of approximately 10 dB when using the IIR section.

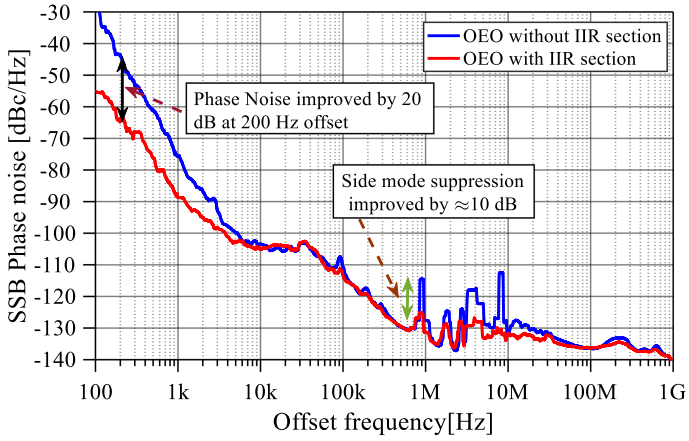

Fig. 4. Phase noise of the generated RF signal using the tunable OEO at 17.33 GHz. There is approximately 10 dB improvement in SMSR and 20 dB improvement of phase noise at 200 Hz offset frequency when the IIR section is included.

i.e., on the frequency response of the various optical and electrical components that comprise the OEO loop. The characteristics of the generated RF signals are described below, for two scenarios, namely the OEO with and without the IIR MWP filter section. For the latter case, which corresponds to the scenario described in [13], we removed the IIR section (corresponding to the red dotted box in Fig. 1).

The electrical spectrum of the generated RF signal at the oscillation frequency of 17.33 GHz for the OEO without and with the IIR section are shown in Fig. 3(a) and Fig. 3(b) respectively. Side-modes at integer multiples of an offset of approximately 1 MHz were observed around the carrier, which originate from the fiber delay line of length 200 m. The IIR section in the OEO suppresses the side modes by an additional 10 dB as compared to the OEO without the IIR section that was reported in [13]. This improvement is due to the enhancement of the Q factor of the OEO loop that results from cascading the tunable single passband section with the IIR section. The suppression effect is also discernable in the phase noise plot as shown in Fig. 4, where inclusion of the IIR section leads to a 20 dB reduction of the SSB phase noise close to carrier (at an offset frequency of 200 Hz). Again, the postulated reason behind the phase noise improvement is due to the Q factor improvement which is supported by the second term of the Leeson formula for

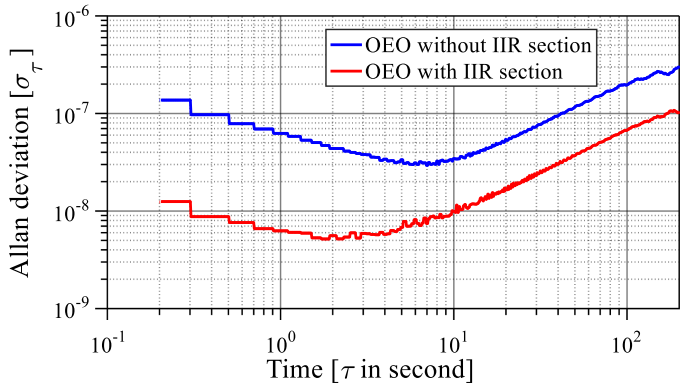

Fig. 5. Measured Allan deviation of the OEO generated RF signal at 17.33 GHz. The frequency stability is 6.1 $\times$ 10^{-9} at 1 s.

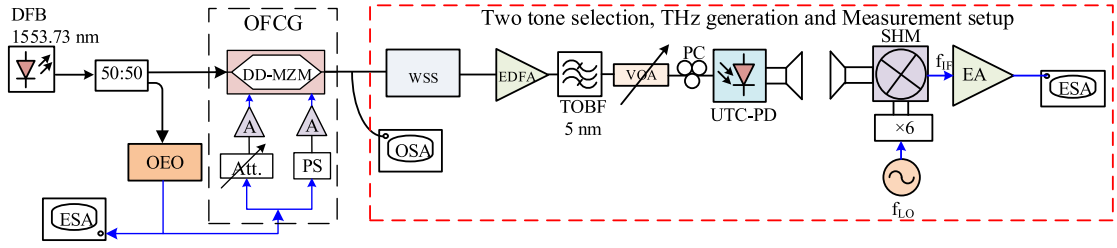

Fig. 6. Experimental arrangement for THz signal generation, with the OEO implemented according to Fig. 1.

oscillator phase noise [21]:

$$L(f_m) = 10\log_{10}\left[\left(\frac{FkT}{2P_{in}}\right)\left(1+\frac{{f_0}^2}{(2f_mQ_L)^2}\right)\left(1+\frac{f_c}{f_m}\right)\right] \tag{3}$$

Here f_m is the offset frequency, f_0 is the oscillation frequency, f_c is the $1/f$ corner frequency, F is the active device noise factor, Q_L is the loaded quality factor of the loop and P_{in} is the RF power input to the amplifier. The Q factor of the optoelectronic loop fundamentally determines the close-to-carrier phase noise. The noise floor is determined by the shot noise power of the photo-detector [22], and this is essentially the same for both arrangements since the parameters that determine the noise floor are identical for the OEO with and without the IIR MWP filter section. As shown in Fig. 4, the SSB phase noise is less than -103 dBc/Hz at 10 kHz offset for the both cases. From Fig. 4, it is seen that by using the cascaded MWP filter, the side modes are suppressed by 125 dB. We then examined the Allan deviation, which is used to express the frequency stability of an oscillator. The measured Allan deviation for two different OEO scenarios is depicted in Fig. 5. The OEO with the IIR section has better frequency stability as compared to that without the IIR section [13]. The Allan deviation of the OEO with the IIR section is 6.1 $\times$ 10^{-9} at 1s observation time which signifies that there exists a 105 Hz frequency drift between two observations that are 1 s apart which is ten times lower than the frequency drift of [13], for which the frequency drift is around 1 kHz at 1 s.

4. Side Mode Suppressed Thz Signal Generation

We generated a THz signal by using the OEO as an RF source for an optical frequency comb generator (OFCG) via two-tone selection and optical heterodyning techniques as shown in Fig. 6. The optical frequency comb shown in Fig. 7 was generated by driving the two RF ports of a dual

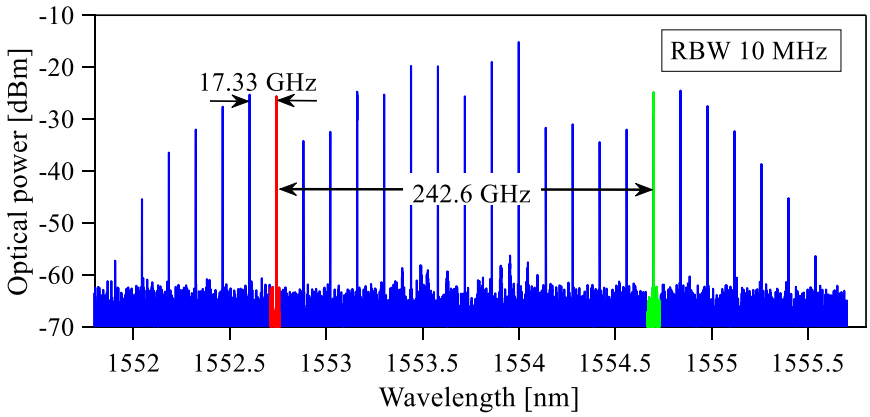

Fig. 7. Optical spectrum of the generated comb with a spacing of 17.33 GHz. The tones marked in red and green were selected for THz signal generation at 242.6 GHz using the WSS in the experimental arrangement of Fig. 6.

drive Mach Zehnder modulator (DD-MZM, Photonic Systems Inc. PSI-3600-MOD) with RF signals of different amplitudes and phases [23], [24]. The black dotted box of Fig. 6 shows the detailed construction of the OFCG. We selected two comb lines (using a wavelength selective switch (WSS)) and generated a THz signal of 242.6 GHz though beating in a UTC-PD. Before heterodyning in the UTC-PD, the two tones selected with the WSS (Finisar WaveShaper, 4000S) were amplified with an EDFA, filtered by a 5 nm optical bandpass filter and then controlled using a variable optical attenuator (VOA). The UTC-PD is an unpackaged device which was connected to a horn antenna (20 dBi) via a coplanar mm-wave probe. Another identical horn antenna was used to receive the transmitted THz signal over a 30 cm wireless path.

The received THz signal was then down-converted by mixing it in a sub-harmonic mixer (SHM) with the signal generated from a Rohde & Schwarz synthesizer (SMA100A) which was used as a local oscillator (LO). Prior to connecting it to the SHM, the LO signal frequency was multiplied by a factor of six; a SHM (Virginia Diodes, Inc. VDI WR3.4SHM) was used to mix the second harmonic of the electrical multiplier's output with the received THz signal. The mixer's intermediate frequency (IF) was adjusted to be within the operating range of the microwave components and instruments by varying the LO frequency. The IF signal was then electrically amplified (using an RF-Lambda RLNA00G30GA amplifier) prior to connection to an ESA. The electrical spectra of the down-converted signal for the two OEO arrangements are shown in Fig. 8(a) for the system without the IIR MWP filter section and in Fig. 8(b) for the situation in which the IIR filter is included. As we can see from Fig. 8(a), both the primary side modes (spaced approximately 1 MHz around the carrier) and secondary side modes (spaced approximately 100 kHz around the primary side modes) of the OEO generated microwave signal are translated in the THz signals. When the IIR MWP filter section is included in the driving OEO the side modes both in the generated microwave signal and the THz signal are suppressed, as seen in Fig. 8(b).

5. RoF link Based on Cascaded MWP Filter Based OEO Driven OFCG

Finally, we implemented a radio over fiber (RoF) link at 242.6 GHz using the cascaded MWP filter based OEO driven OFCG. The experimental set-up for the RoF link is illustrated in Fig. 9. Here, the electrical signal generated by the OEO section (as described in Section 3) was used to drive the OFCG (discussed in section 4). An EDFA was used to amplify the output of the OFCG (optical spectrum as in Fig. 7) prior to connection to a WSS (Finisar WaveShaper, 4000S). Two comb lines (the red and green lines of Fig. 7) were selected and directed to two different output ports of the WSS, with the output of one port being used as a local oscillator (LO) signal while the other line was

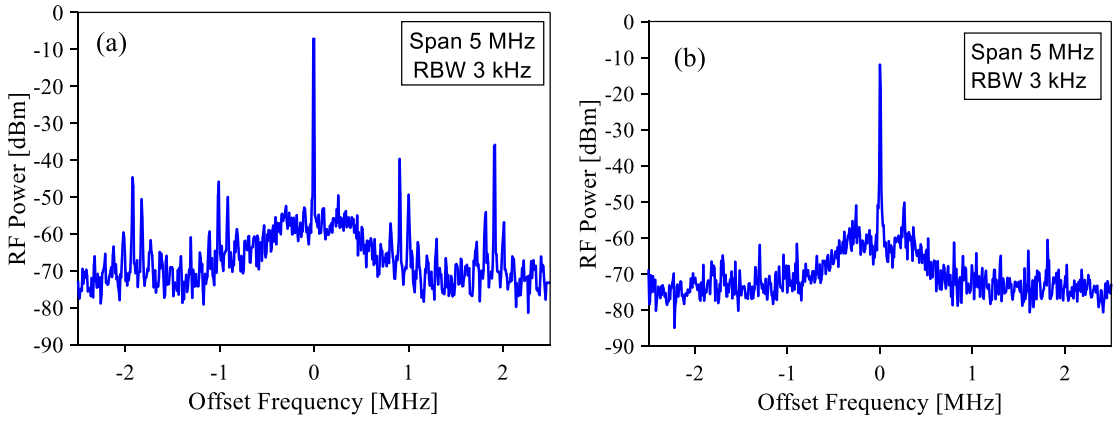

Fig. 8. Electrical spectrum of the down-converted signal with center frequency at (a) 14.82 GHz without IIR section and (b) 8.43 GHz with IIR section in the driving OEO.

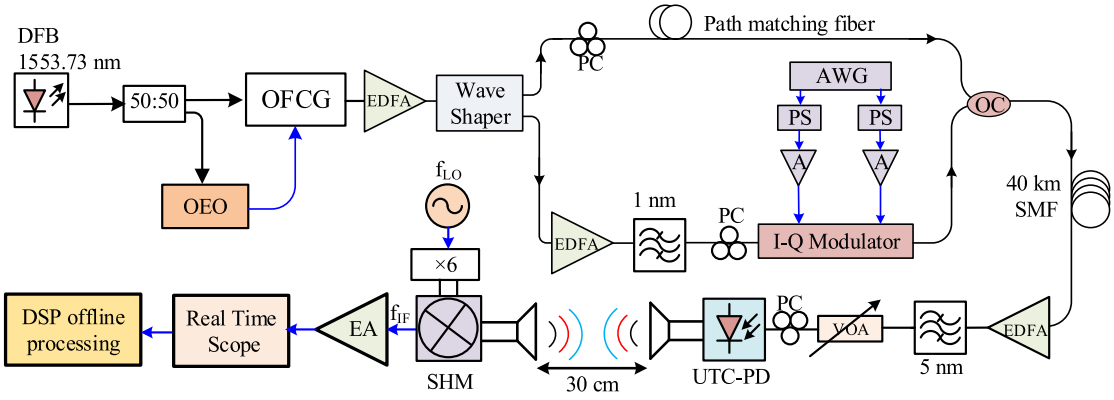

Fig. 9. Experimental set-up of the radio over fiber link. The optical paths are represented by black line while the electrical paths are represented by blue line.

used for data modulation. Prior to connection to an I-Q modulator, the optical signal was amplified by another EDFA and subsequently an optical filter (1 mn) was used to filter out the stimulated emission (ASE) noise. A Tektronix arbitrary waveform generator (AWG7000, with a sampling rate of 50 GSa/s) was used to generate the modulation signal which was further amplified electrically and phase sifted prior to the I-Q modulator.

In the LO tone path, a path matching SMF of 39.5 m was added to balance the path difference with the modulated tone path. A 50:50 optical coupler was used to combine the LO optical tone and the modulated tone, with the combined output being transmitted through a 40 km SMF and amplified by an EDFA. ASE noise from EDFA was eliminated by a 5 nm optical filter. We used an UTC-PD for optical to electrical (O/E) conversion; a VOA, placed before the UTC-PD, was used to control the input optical power. A pair of horn antennas (each of 20 dBi gain) were used to transmit and receive the data-modulated THz signal generated at the output of the UTC-PD over a 30 cm wireless path. The received THz signal was then down-converted by a SHM and electrical local oscillator combination, amplified by electrical amplifier (EA), captured by a digital real time oscilloscope (36 GHz bandwidth and sampling rate of 80 GSa/s), and subsequently processed by a MATLAB offline digital signal processor (DSP). Polarization controllers (PC) were used in different parts of the set-up to minimize the polarization dependent losses and to align the polarization with the functioning component. In the DSP processing unit, the signal was first down-converted and

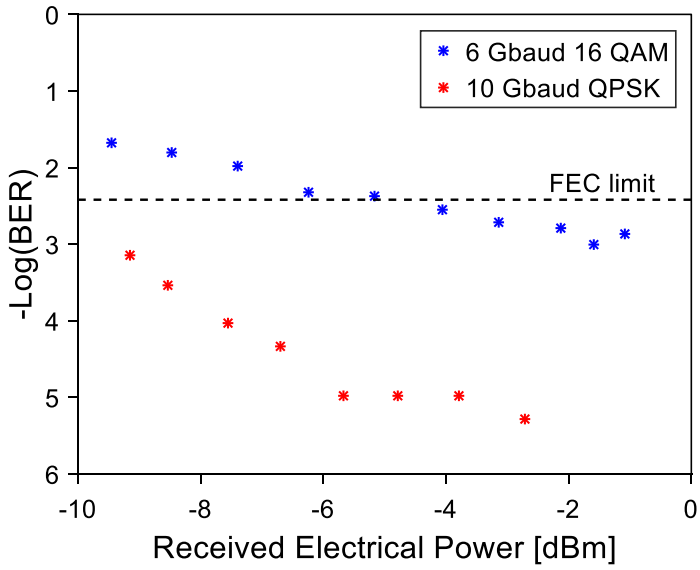

Fig. 10. BER at different received electrical power of the radio over fiber link.

resampled. Then the resampled signal was passed through a channel equalizer, a frequency offset estimator and a carrier phase estimator. Finally, the BER was evaluated. The BER as a function of received electrical power is depicted in Fig. 10 for two different modulation formats. As seen from Fig. 10, the BER is below the forward error correction (FEC) limit of 3.8×10^{-3} for 7% overhead bits with the data rate of 24 Gbps for 6 Gbaud 16 QAM and 20 Gbps for 10 Gbaud QPSK modulation.

6. Conclusion

We have demonstrated a highly side mode suppressed optoelectronic oscillator by employing a microwave photonic filter which is realized by cascading a single passband filter and an optoelectronic IIR filter. The experimental results show that incorporating the IIR MWP filter section in the OEO improves the side mode suppression by 10 dB, and the close to carrier phase noise by 20 dB compared to the corresponding implementation without the IIR section in place. Inclusion of the IIR section also enhances side mode suppression when the OEO is used to drive an OFCG for THz signal generation. A RoF link was implemented as an application scenario of the proposed system.

References

[1] M. F. Lewis, "Novel RF oscillator using optical components," *Electron. Lett.*, vol. 28, no. 1, pp. 31–32, Jan. 1992.
[2] X. S. Yao and L. Maleki, "Optoelectronic microwave oscillator," *J. Opt. Soc. Amer. B*, vol. 13, no. 8, pp. 1725, Aug. 1996.
[3] X. Zou *et al.*, "Optoelectronic oscillators (OEOs) to sensing, measurement, and detection," *IEEE J. Quantum Electron.*, vol. 52, no. 1, pp. 1–16, Jan. 2016.
[4] Y. Wang, J. Zhang, and J. Yao, "An optoelectronic oscillator for high sensitivity temperature sensing," *IEEE Photon. Technol. Lett.*, vol. 28, no. 13, pp. 1458–1461, 2016.
[5] H. Yu *et al.*, "Simple photonic-assisted radio frequency down-converter based on optoelectronic oscillator," *Photon. Res.,* vol. 2, no. 4, pp. B1, Aug. 2014.
[6] D. Lu, B. Pan, H. Chen, and L. Zhao, "Frequency-tunable optoelectronic oscillator using a dual-mode amplified feedback laser as an electrically controlled active microwave photonic filter," *Opt. Lett.*, vol. 40, no. 18, pp. 4340–4343, 2015.
[7] M. Fleyer, A. Sherman, M. Horowitz, and M. Namer, "Wideband-frequency tunable optoelectronic oscillator based on injection locking to an electronic oscillator," *Opt. Lett.*, vol. 41, no. 9, pp. 1993–1996, 2016.
[8] T. Chen, X. Yi, L. Li, and R. Minasian, "Single passband microwave photonic filter with wideband tunability and adjustable bandwidth," *Opt. Lett.*, vol. 37, no. 22, pp. 4699–4701, 2012.
[9] L. Cheng and S. Aditya, "A novel photonic microwave filter with infinite impulse response," *IEEE Photon. Technol. Lett.*, vol. 19, no. 19, pp. 1439–1441, 2007.

[10] G. Charalambous, G. K. M. Hasanuzzaman, A. Perentos, and S. Iezekiel, "Optoelectronic recirculating delay line implementation of a high-Q optoelectronic oscillator," in *Proc. Int. Topical Meeting Microw. Photon.*, 2017, pp. 1–4.
[11] A. Liu *et al.*, "Spurious suppression in millimeter-wave OEO with a High-Q optoelectronic filter," *IEEE Photon. Technol. Lett.*, vol. 29, no. 19, pp. 1671–1674, 2017.
[12] H. Tang, Y. Yu, Z. Wang, L. Xu, and X. Zhang, "Wideband tunable optoelectronic oscillator based on a microwave photonic filter with an ultra- narrow passband," *Opt. Lett.*, vol. 43, no. 10, pp. 2328–2331, May 2018.
[13] G. Hasanuzzaman, H. Shams, C. Renaud, J. Mitchell, A. Seeds, and S. Iezekiel, "Tunable THz signal generation and radioover-fiber link based on an optoelectronic Oscillator-driven optical frequency comb," *J. Lightw. Technol.*, vol. 38, no. 19, pp. 5240–5247, 2020.
[14] W. Zhou and G. Blasche, "Injection-Locked dual opto-electronic oscillator with ultra-low phase noise and ultra-low spurious level," *IEEE Trans. Microw. Theory Tech.*, vol. 53, no. 3, pp. 929–933, 2005.
[15] Y. Jiang, J. Yu, Y. Wang, L. Zhang, and E. Yang, "An optical domain combined dual-loop optoelectronic oscillator," *IEEE Photon. Technol. Lett.*, vol. 19, no. 11, pp. 807–809, 2007.
[16] M. Bagnell, J. Davila-Rodriguez, and P. J. Delfyett, "Millimeter-wave generation in an optoelectronic oscillator using an ultrahigh finesse etalon as a photonic filter," *J. Lightw. Technol.*, vol. 32, no. 6, pp. 1063–1067, 2014.
[17] L. Bogataj, M. Vidmar, and B. Batagelj, "Opto-electronic oscillator with quality multiplier," *IEEE Trans. Microw. Theory Tech.*, vol. 64, no. 2, pp. 663–668, 2016.
[18] Y. Jiang *et al.*, "Frequency locked single-mode optoelectronic oscillator by using low frequency RF signal injection," *IEEE Photon. Technol. Lett.*, vol. 25, no. 4, pp. 382–384, 2013.
[19] G. Ning, L. H. Cheng, S. Aditya, P. Shum, and J. Q. Zhou, "Infinite impulse response microwave photonic filter using a dual drive modulator with an optoelectronic feedback loop," *J. Mod. Opt.*, vol. 55, no. 14, pp. 2293–2299, 2008.
[20] G. Ning, L. Cheng, S. Aditya, J. Zhou, and P. Shum, "General analyses of infinite impulse microwave photonic filters with an intensity modulator in an opto-electronic feedback loop," *Appl. Phys. B Lasers Opt.*, vol. 92, no. 4, pp. 609–614, 2008.
[21] T. H. Lee and A. Hajimiri, "Oscillator phase noise: A tutorial," *IEEE J. Solid-State Circuits*, vol. 35, no. 3, pp. 326–335, 2000.
[22] L. Maleki, "The opto-electronic oscillator (OEO): Review and recent progress," in *Proc 2012 Eur. Freq. Time Forum*, 2012, pp. 497–500.
[23] T. Sakamoto, T. Kawanishi, and M. Izutsu, "Asymptotic formalism for ultraflat optical frequency comb generation using a Mach-Zehnder modulator," *Opt. Lett.*, vol. 32, no. 11, pp. 1515–1517, 2007.
[24] H. Shams *et al.*, "Sub-THz wireless over fiber for frequency band 220-280 GHz," *J. Lightw. Technol.*, vol. 34, no. 20, pp. 4786–4793, Oct. 2016.